Journal of Photochemistry and Photobiology A: Chemistry 202 (2009) 154–158

Contents lists available at ScienceDirect

Journal of Photochemistry and Photobiology A: Chemistry

journal homepage: www.elsevier.com/locate/jphotochem

Study of visible light photocatalytic activity achieved by NMP solvent treatment of polymorphic titania

Sujaree Kaewgun, Daniel Mckinney, Jamie White, Andrew Smith, Michael Tinker, Josh Ziska, Burtrand I. Lee*

School of Materials Science and Engineering, Clemson University, Clemson, SC 29634, USA

ARTICLE INFO

Article history:
Received 16 July 2008
Received in revised form
28 September 2008
Accepted 1 December 2008
Available online 11 December 2008

Keywords:
Polymorphic titania
Brookite
Visible light
Methyl orange
Photocatalytic activity

ABSTRACT

Visible light active polymorphic titania samples were prepared by post-treatment of a water-based ambient condition sol (WACS) sample using a solvent-based ambient condition sol (SACS) process with N-methylpyrrolidone (NMP) as the solvent. SACS samples were calcined in either air or nitrogen atmosphere under various conditions. Nitrogen incorporation of SACS titania was investigated by CHN analysis and X-ray photoelectron spectroscopy (XPS). All samples were also characterized by X-ray diffraction, N_2 physisorption, UV/Vis absorption spectroscopy, and TEM and compared to a commercial titania powder, Degussa P25. The calcination conditions, especially the temperature and calcination atmosphere, have an influence on the BET surface area, crystallite size, titania phase content, and photocatalytic activity, evaluated by the degradation of methyl orange dye under visible light irradiation. SACS calcined in air at 200 °C for 2 h showed the best visible light activated photocatalytic performance in this study.

1. Introduction

It is known that titania is activated by ultraviolet (UV) light for photocatalytic reactions. However, visible light (VL), wavelengths ~400–700 nm, is the major fraction (about 45%) of solar radiation which has only 5% of UV with the remaining for infrared [1]. The band gap of titania is about 3.2 eV, which can only absorb wavelengths shorter than 388 nm, which is out of the VL region. For efficient utilization of solar energy by titania photocatalysts, narrowing its band gap to VL energy range is required. Many researchers have studied visible light active (VLA) anatase and rutile titania by doping the titanias with transition metals such as Fe^{3+}, Mo^{5+}, Ru^{3+}, Os^{3+}, Re^{5+}, V^{4+}, or Rh^{3+}, or non-metals such as N, C, F, P, or S to narrow their band gap. Asahi et al. [2] claimed that anionic doping is superior to metal cation doping since metal cations often give localized *d* states deep in the band gap of titania but create new recombination centers of e^--h^+. They reported that N-doped anatase titania showed higher photodegradation activities of methylene blue and gaseous acetaldehyde than un-doped titania under VL (wavelength < 500 nm) [2]. They accounted for the improvement by N-substitution into oxygen sites of titania. The substitutional N doping was the most effective among other non-metals doping since its p states contribute to the band gap narrowing by mixing with O 2p states. However, only a few papers on VLA brookite titania were found [3,4]. Recently, many studies have been reported on preparation of nitrogen doped titania by using various techniques such as annealing under a gaseous NH_3 flow [5], sputtering TiO_2 in N_2 gas [2], using an aqueous ammonia solution [6], urea [7], an amine precursor solution [8], or a solvothermal treatment in N precursor solvents [3,9,10].

Our previous solvothermal titania study [9] reported that the solvent-based ambient condition sol (SACS) process, using N-methylpyrrolidone (NMP) as the solvent, enhanced the photocatalytic activities of polymorphic titania under VL irradiation. The nitrogen atoms contained in NMP, when incorporated with titania, narrowed the band gap of titania. The preliminary results showed that the calcination temperatures affected BET surface area, particle size, titania phase content, and photocatalytic activities. The results presented below are from further examination of the influence of calcination conditions, i.e., calcination atmosphere, temperature, and time. The physical properties with nitrogen incorporation in all titania samples are reported. The photocatalytic activities under VL exposure, evaluated by the degradation of methyl orange (MO) dye, are presented with that of a commercial reference titania, Degussa P25.

2. Experimental

Polymorphic titania was prepared by the water-based ambient condition sol (WACS) process, using titanium tetrachloride ($TiCl_4$)

* Corresponding author. Tel.: +1 864 6565348; fax: +1 864 656 1453.
E-mail address: burt.lee@ces.clemson.edu (B.I. Lee).

1010-6030/$ – see front matter © 2008 Elsevier B.V. All rights reserved.
doi:10.1016/j.jphotochem.2008.12.003

Table 1
Experimental conditions used to produce polymorphic titania and % content of titania phase.

Sample ID	% Content of TiO_2 phase (wt%)[a]			Mode of formation	Preparation or post-treated temperature (°C)	Preparation or post-treated time (h)
	An	Br	Ru			
WACS	48	50	2	WACS	83	15
WACS-200	45	53	2	Calcination of WACS	200	2
SACS	42	55	3	SACS of WACS	170	4
SACS-200/2/A	44	53	3	Calcination of SACS in air	200	2
SACS-200/4/A	45	52	3			4
SACS-200/6/A	46	52	2			6
SACS-300/2/A	45	51	4		300	2
SACS-400/2/A	28	65	7		400	2
SACS-200/2/N	45	52	3	Calcination of SACS in nitrogen	200	2
SACS-200/4/N	47	51	2			4
SACS-200/6/N	42	56	2			6
SACS-300/2/N	41	57	2		300	2
SACS-400/2/N	34	63	3		400	2
P25	79	–	21	High T flame oxidation	N/A	N/A

[a] Obtained from XRD data; An, anatase; Br, brookite; Ru, rutile.

in a 1:2 ratio of water–isopropanol system with 0.3 M hydrochloric acid under a refluxing condition as described in our previous papers [11–13]. The WACS samples were calcined in air at 200 °C for 2 h. A solvothermal post-treatment, or SACS [9,14–16], was applied to modify the WACS samples. The SACS process was carried out in N-methylpyrrolidone (NMP) at 170 °C for 4 h in a sealed Teflon container followed by calcination in either air or nitrogen at 200 °C for 2, 4, or 6 h and also at 300 °C and 400 °C for 2 h. The nomenclature, preparation conditions, and percent phase composition of titania samples are given in Table 1.

Phase composition and crystallite size of all samples were determined, as shown in our previous reports [9,14,17], by X-ray diffractometry (XRD) using XDS 2000, Scintag PAD V utilizing Cu Kα radiation at 1.5406 Å, measured with a step size of 0.020° over a range of 20–35°, and a 2θ angular region. The BET surface area, pore volume, and average pore diameter of the samples were determined by N_2 physisorption at −196 °C using a Micromeritics ASAP 2020 automated system. The amount of nitrogen in the titania samples was determined using a CHN analyzer (PerkinElmer 2400 SeriesII). The chemical states of species in the TiO_2 samples were investigated using X-ray photoelectron spectroscopy (XPS), employing Kratos XPS with a monochromatic Al Kα X-ray source system. Light absorbance of the titania samples were recorded using a UV/Vis spectrophotometer of GretagMacbeth Color i5 across a UV/Vis range of 360–750 nm.

The photocatalytic activities of TiO_2 samples were evaluated by observing the photocatalytic degradation of the MO under VL irradiation with wavelength at 560–612 nm. The MO test experiment followed the procedure found in the literatures [9,13,14]. Titania samples of 0.2 g were added to 100 ml of 20 μM MO solution, and then stirred for 30 min without VL exposure and continuously stirred throughout the reaction. A sample was taken every 30 min, then the titania particles were separated from the MO solution by vacuum filtration to prevent scattering. A compact fluorescent lamp (Philips energy saver 60 soft white A19, 14 W) was used as the VL source. The quantitative spectral results of MO were monitored by a UNICAM UV/vis spectrophotometer (Model: 5625). The MO degradation percent value, D, was calculated by Eq. (1).

$$D = \frac{A_0 - A}{A_0} \times 100\% \quad (1)$$

where, A_0 is the initial 490 nm absorbance peak intensity and A is the instantaneous 490 nm peak intensity [9,13,14].

3. Results and discussion

XRD patterns of all SACS samples are given in Fig. 1. The calculated percent of TiO_2 phases from XRD data are shown in Table 1. The phase composition of uncalcined WACS and SACS and calcined SACS at 200–300 °C varied as follows: 50–55% brookite, 40–48% anatase, and a small amount of rutile (less than 5%). The crystallinity of the prepared WACS and post-treatment SACS samples was relatively similar, as obtained from the XRD pattern. The proportion of brookite and rutile in the structure increased for calcined SACS at 400 °C either in air or N_2 atmospheres. The crystallite size in Table 2, calculated from the XRD data using the Scherrer equation, of all prepared titania samples ranged from 5 to 10 nm, which is approximately 3 times smaller than that of P25. This agrees well

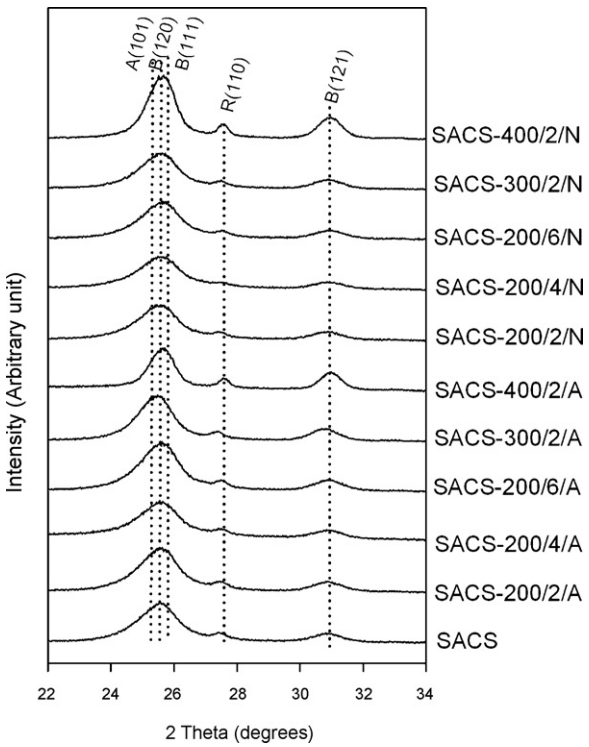

Fig. 1. The XRD patterns of the prepared titania samples and P25 (A = anatase, B = brookite, and R = rutile).

Table 2
The physical properties of as-prepared titania and the reference P25.

Sample ID	Crystallite size (nm)[a]			BET surface area (m^2/g)[b]	Pore volume (cm^3/g)[b]	Pore size average (Å)[b]	Doped N content (wt%)[c]
	Anatase	Brookite	Rutile				
WACS	6	8	19	163	0.1	25	0
WACS-200	6	7	18	157	0.1	27	0
SACS	7	8	12	133	0.1	24	0.09
SACS-200/2/A	6	8	11	138	0.1	25	0.16
SACS-200/4/A	6	9	11	171	0.1	24	N/A
SACS-200/6/A	5	7	19	172	0.1	25	0.12
SACS-300/2/A	6	8	13	143	0.1	29	0
SACS-400/2/A	8	10	20	68	0.1	60	0
SACS-200/2/N	5	8	14	139	0.1	24	0.77
SACS-200/4/N	5	7	14	128	0.1	24	N/A
SACS-200/6/N	5	9	19	118	0.1	24	0.13
SACS-300/2/N	5	9	13	114	0.1	27	0.33
SACS-400/2/N	9	10	21	82	0.1	42	0.01
P25	21	–	40	56	0.2	169	0

[a] Calculated from XRD data using the Scherrer equation. Error of measurement = ± 5%.
[b] Using N_2 physisorption at −196 °C. Error of measurement = ± 10%.
[c] Determined by CHN analyzer.

with the size determined by TEM micrographs which was reported in our previous work [9]. However, the rutile phase, which is very small in proportion within the prepared titania polymorph, shows the crystallite size ~10–20 nm.

BET surface areas, pore volume, and average pore diameter of the titania samples are given in Table 2. The surface area of as-prepared titania samples is approximately 3 times larger than that of P25 sample. The surface area of SACS, SACS-200/2/A, and SACS-200/2/N samples were similar, approximately 15–20% less than that of WACS and WACS-200 samples. It can be explained that calcination at 200 °C for 2 h in either air or N_2 could not completely remove residual NMP on the titania surface. In Fig. 2, the surface area of calcined SACS samples in N_2 atmosphere shows a decreasing trend with increasing calcination temperature and time. This is attributable to the sintering of titania nanoparticles and the residual decomposition products of NMP by the heat treatment. On the other hand, the surface area of calcined SACS samples in air for 4 and 6 h increased approximately 24% from those calcined for 2 h. Unlike the calcination in nitrogen, some of NMP was oxidized and removed from the titania surface by the heating in oxidizing atmosphere. At a higher calcination temperature of 400 °C in air, the surface area reduced by 50% because of the sintering.

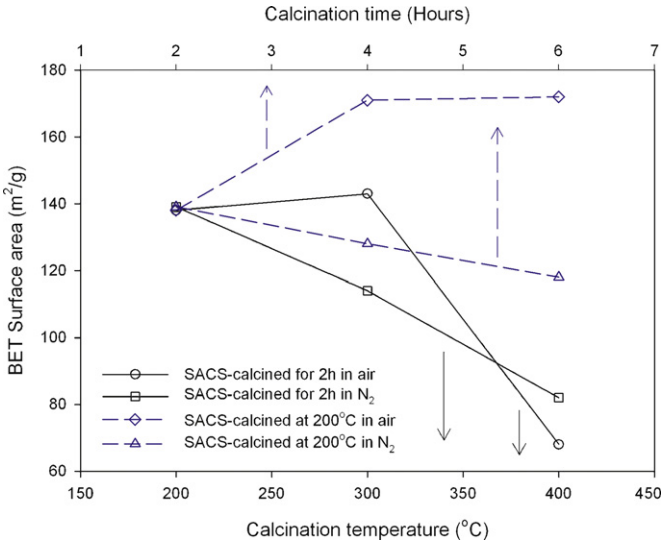

Fig. 2. The effect of calcination temperature and time for SACS samples on BET surface area.

Fig. 3(a) exhibits nitrogen content and Fig. 3(b) presents carbon and hydrogen contents, obtained from CHN analysis, of calcined SACS samples as a function of both calcination temperature and time. The nitrogen, carbon, and hydrogen contents decreased with increasing the temperature and time of calcination in either air or nitrogen. Some of N, C, and H have been volatilized, expectedly more from air calcination. SACS-200/2/N has approximately 5 times more nitrogen content than SACS-200/2/A, since nitrogen in the SACS

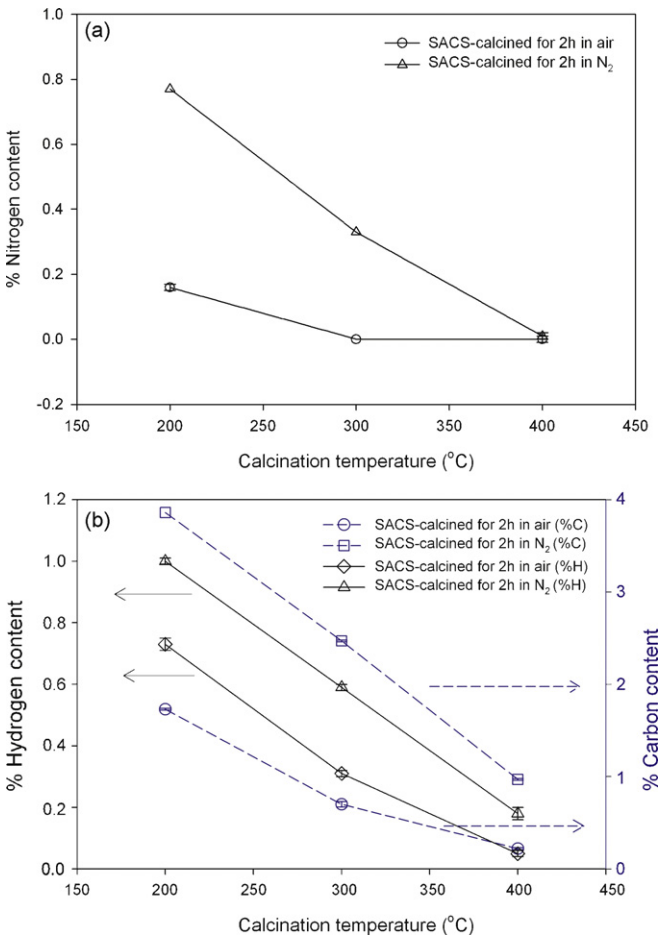

Fig. 3. The effect of calcination temperature for SACS samples on (a) nitrogen content, and (b) carbon and hydrogen content.

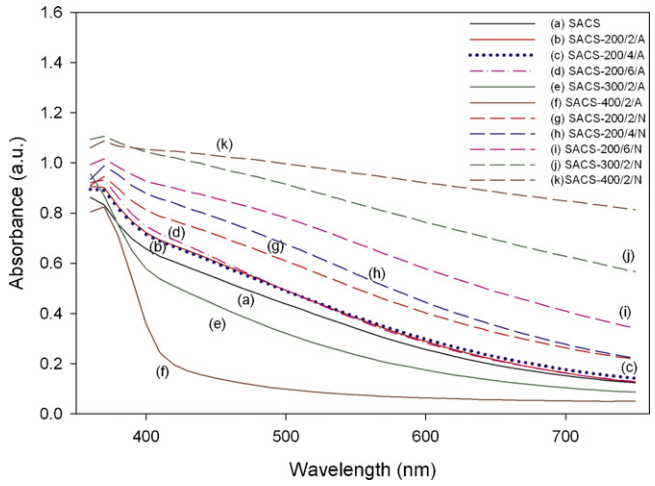

Fig. 4. UV/Vis spectra of as-prepared SACS samples.

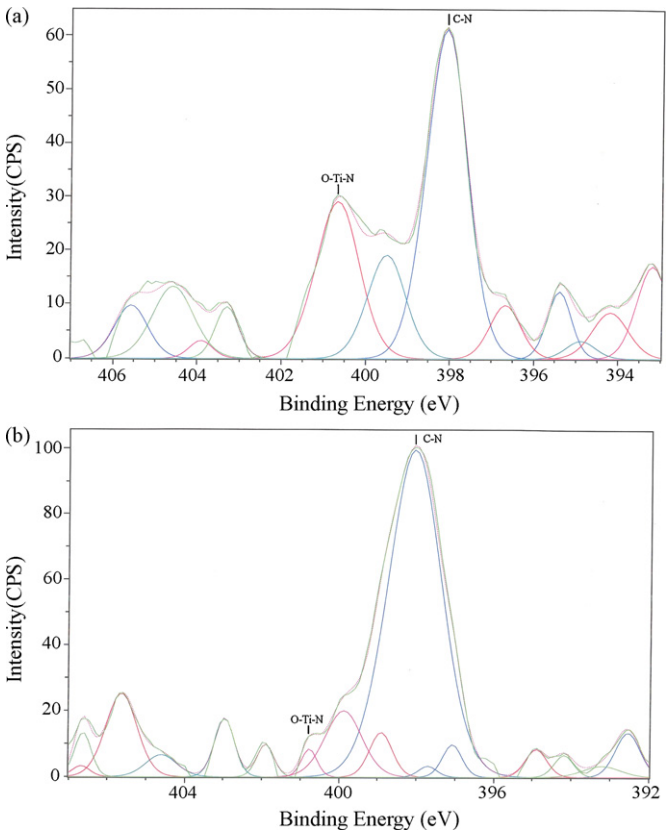

Fig. 5. N 1s XPS spectrum of (a) SACS-200/2/A, and (b) SACS-200/2/N.

samples was oxidized by O_2 gas in air atmosphere. Nitrogen was completely released when calcined at a temperature above 300 °C in air and 400 °C in nitrogen.

Fig. 4 shows UV/Vis spectra of titania samples. SACS samples exhibited shift of the absorption shoulders to the VL region, compared with P25 and WACS-200 in the previous study [9]. The shifting of absorption shoulders of all SACS samples calcined in nitrogen is greater than the WACS-200 and P25. The SACS samples calcined in air showed less absorption since much of the doped nitrogen was released by the reoxidation [6]. In the case of SACS calcined in nitrogen, the greater shifting was observed with increasing calcination time and temperature. On the other hand, the absorption shoulders shifting of SACS calcined in air with increasing calcination time was similar, but dramatically decreased with increasing calcination temperature. In the case of calcination in air, CHN analysis results in Fig. 3 depict that the more N in the structure with decreasing calcination temperature, the greater the VL absorption. The shifting of absorption shoulders to VL region, or a narrowing of titania band gap, occurs because of N atoms in the SACS samples [2,5–8,18–23]. The greater contribution, however, must come from the partially decomposed NMP remaining as charred organic.

The chemical state of nitrogen in SACS samples calcined in air and nitrogen was examined using XPS as shown in Fig. 5(a) and (b). N 1s XPS during the oxidation process of TiN was investigated by Saha and Tompkins [24] and assigned the peaks as atomic β-N at 396 eV and molecularly chemisorbed γ-N_2 at 400 and 402 eV. However, the N peak at 396 eV was not always present [25]. The XPS spectrum of SACS-200/2/A in Fig. 5(a) reveals three N 1s peak at 398.1, 399.5, and 400.7 eV. Fig. 5(b) is the N 1s XPS peak of SACS-200/2/N revealing two peaks at binding energies of 398.1, and 399.9 eV. The main N 1s peak at 398.1 is attributed to C–N bonds, anionic azide (N_3^-), or NH_3 [26–28]. The peak at ~400 eV is for the N atom in the environment of O–Ti–N or the presence of hyponitrite which is responsible for the VLA photocatalysis [25,29]. This N peak at ~400 eV was also attributed to the doping of the nitrogen into the TiO_2 [25,30]. Both SACS samples contained N 1s peak at 399–401 eV; however, the value of the peak height ratios of O–Ti–N to C–N of SACS-200/2/A is greater than that of SACS-200/2/N.

The photocatalytic activities of the as-prepared titania samples compared to the reference P25, determined by the MO degradation under VL irradiation, are given in Fig. 6(a) and (b). For the sake of discussion and comparison of the reaction times between samples, 80% of MO degradation is arbitrarily set. The results exhibit that SACS samples calcined in air and nitrogen at 200 °C are all VLA. The MO degradation by SACS samples calcined in both atmospheres at 200 °C is 2–3 times faster than the MO degradation for the samples calcined at 300 °C. SACS-200/2/A exhibits the highest photocatalytic activity among the other titania samples. SACS-400/2/A, SACS-400/2/N, WACS-200, and P25, which have no nitrogen, are not VLA as expected. The photocatalytic results of SACS calcined in air were supported by UV/Vis spectra and CHN analysis. The more nitrogen present in SACS calcined in air, the higher the photocatalytic activity. The photocatalytic activities of SACS samples, calcined in nitrogen at various temperatures as shown in Fig. 6(b), increased in the following order: SACS-200/2/N ≅ SACS-200/4/N ≅ SACS-200/6/N > SACS > SACS-300/2/N » SACS-400/2/N. The VL activity trend of SACS calcined in nitrogen was inconsistent with the UV/Vis absorbance in Fig. 4. For example, according to UV/Vis absorbance, SACS-400/2/N should be the most VLA sample. These results indicate that VL photocatalytic performance is not directly related to the VL absorbance [6]. Moreover, the much lower photocatalytic activities of SACS calcined at temperatures above 200 °C can be attributed to the significantly lower BET surface area. In the case of calcination at 200 °C for 2 h, MO degradation with SACS calcined in air is 2 h faster than when calcined in nitrogen, even though SACS-200/2/A contained about 5 times less nitrogen than SACS-200/2/N. This result has two possible explanations. First, not all states of nitrogen in titania are VLA. There is more nitrogen in the form of hyponitrite [25,29], which is required for VL photocatalysis, in SACS-200/2/A than in SACS-200/2/N. Additionally, it has been suggested that the partial release of doped nitrogen is necessary for samples to appear to be VLA [6]. By varying the time for 200 °C calcination in both air and nitrogen atmospheres, results were obtained that showed calcination time have little influence on photocatalytic activities in nitrogen atmosphere. Contrarily, when SACS samples were calcined in air for various times, the photocatalytic activity declined

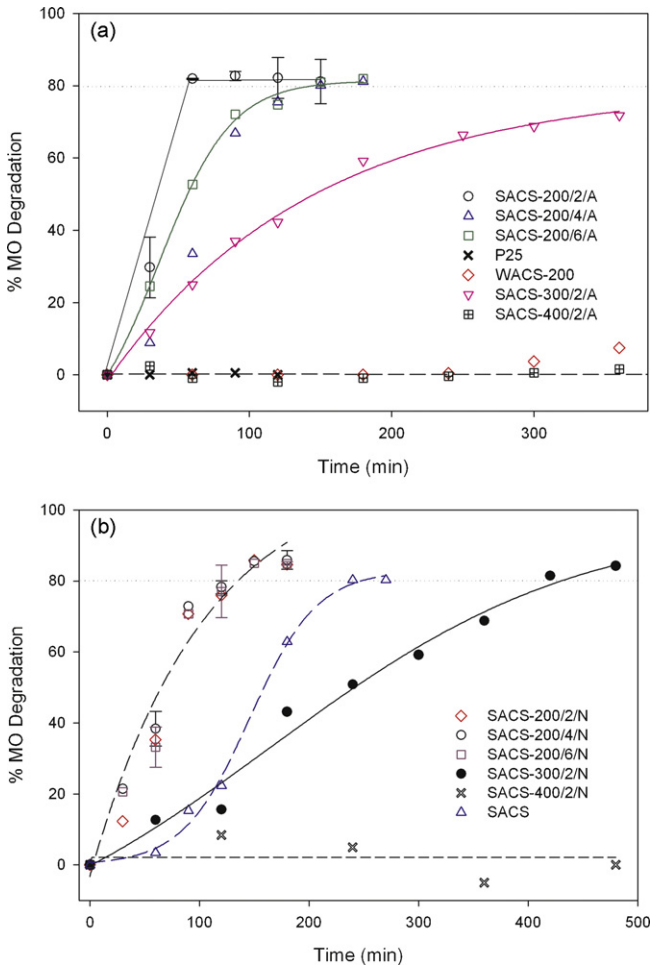

Fig. 6. MO degradation under VL irradiation of (a) SACS samples calcined in air compared to WACS-200 and commercial P25, and (b) uncalcined SACS and SACS samples calcined in nitrogen.

with increasing time after and initial period of 2 h by reducing the content of hyponitrite.

4. Conclusions

A post-treatment, called SACS process with NMP solvent, of as-prepared polymorphic titania, improved the VL photocatalytic activity of the samples. The calcination conditions, i.e., temperature, time, and calcination atmosphere (either air or nitrogen) affected the photocatalytic activities. The photocatalytic activity declined with increasing calcination temperature and time. However, calcination time did not have a significant effect on VLA properties, especially in the SACS samples calcined in nitrogen. SACS-200/2/A showed the best VLA performance, since SACS-200/2/A has greater amount of VLA nitrogen in the form of hyponitrite than that in SACS-200/2/N.

Acknowledgments

This research was supported by the Petroleum Research Fund of American Chemical Society and partially supported by the Creative Inquiry Undergraduate Research Program of Clemson University.

References

[1] J.L. Gole, J.D. Stout, C. Burda, Y.B. Lou, X.B. Chen, J. Phys. Chem. B 108 (2004) 1230–1240.
[2] R. Asahi, T. Morikawa, T. Ohwaki, K. Aoki, Y. Taga, Science 293 (2001) 269–271.
[3] T. Sato, Y. Aita, M. Komatsu, S. Yin, J. Mater. Sci. 41 (2006) 1433–1438.
[4] X. Ye, D. Chen, K. Li, V. Shar, M. Kesmez, K. Vajifdar, Chem. Eng. Commun. 194 (2007) 368–381.
[5] H. Irie, Y. Watanabe, K. Hashimoto, J. Phys. Chem. B 107 (2003) 5483–5486.
[6] T. Matsumoto, N. Iyi, Y. Kaneko, K. Kitamura, S. Ishihara, Y. Takasu, Y. Murakami, Catal. Today 120 (2007) 226–232.
[7] B. Chi, L. Zhao, T. Jin, J. Phys. Chem. C 111 (2007) 6189–6193.
[8] Y. Aita, M. Komatsu, S. Yin, T. Sato, J. Solid State Chem. 177 (2004) 3235–3238.
[9] S. Kaewgun, C.A. Nolph, B.I. Lee, Catal. Lett. 123 (2008) 173–180.
[10] S. Yin, Y. Aita, M. Komatsu, J.S. Wang, Q. Tang, T. Sato, J. Mater. Chem. 15 (2005) 674–682.
[11] R.C. Bhave, B.I. Lee, Mater. Sci. Eng. a-Struct. 467 (2007) 146–149.
[12] B.I. Lee, X.Y. Wang, R. Bhave, M. Hu, Mater. Lett. 60 (2006) 1179–1183.
[13] C.A. Nolph, D.E. Sievers, S. Kaewgun, C.J. Kucera, D.H. McKinney, J.P. Rientjes, J.L. White, R. Bhave, B.I. Lee, Catal. Lett. 117 (2007) 102–106.
[14] S. Kaewgun, C.A. Nolph, B.I. Lee, L.-Q. Wang, Mater. Chem. Phys. J. 2008, in press.
[15] R. Kota, B.I. Lee, J. Mater. Sci.: Mater. Electron. 18 (2007) 1221–1227.
[16] L. Qi, B.I. Lee, P. Badheka, L.Q. Wang, P. Gilmour, W.D. Samuels, G.J. Exarhos, Mater. Lett. 59 (2005) 2794–2798.
[17] H.Z. Zhang, J.F. Banfield, J. Phys. Chem. B 104 (2000) 3481–3487.
[18] S.K. Joung, T. Amemiya, M. Murabayashi, K. Itoh, Appl. Catal. a-Gen. 312 (2006) 20–26.
[19] I.C. Kang, Q.W. Zhang, J. Kano, S. Yin, T. Sato, F. Saito, J. Photochem. Photobiol. A 189 (2007) 232–238.
[20] R. Nakamura, T. Tanaka, Y. Nakato, J. Phys. Chem. B 108 (2004) 10617–10620.
[21] M. Sathish, B. Viswanathan, R.P. Viswanath, C.S. Gopinath, Chem. Mater. 17 (2005) 6349–6353.
[22] N. Venkatachalam, A. Vinu, S. Anandan, B. Arabindoo, V. Murugesan, J. Nanosci. Nanotechnol. 6 (2006) 2499–2507.
[23] S. Yin, Y. Aita, M. Komatsu, T. Sato, J. Eur. Ceram. Soc. 26 (2006) 2735–2742.
[24] N.C. Saha, H.G. Tompkins, J. Appl. Phys. 72 (1992) 3072–3079.
[25] J. Yang, H.Z. Bai, X.C. Tan, J.S. Lian, Appl. Surf. Sci. 253 (2006) 1988–1994.
[26] C. Burda, Y.B. Lou, X.B. Chen, A.C.S. Samia, J. Stout, J.L. Gole, Nano. Lett. 3 (2003) 1049–1051.
[27] X.B. Chen, C. Burda, J. Phys. Chem. B 108 (2004) 15446–15449.
[28] J.F. Moulder, W.F. Stickle, P.E. Sobol, K.D. Bomben, Handbook of X-ray Photoelectron Spectroscopy, Physical Electronics, Inc., MN, USA, 1995.
[29] J.A. Navio, C. Cerrillos, C. Real, Surf. Interface Anal. 24 (1996) 355–359.
[30] S. Sakthivel, H. Kisch, Chemphyschem 4 (2003) 487–490.